Proceedings of the ASME 2010 3rd Joint US-European Fluids Engineering Summer Meeting and 8th International Conference on Nanochannels, Microchannels, and Minichannels
FEDSM-ICNMM2010
August 1-5, 2010, Montreal, Canada

FEDSM-ICNMM2010-30123

MILLI-SCALE JUNCTION FLOW EXPERIMENTS

Evan C. Lemley
Department of Engineering and Physics
University of Central Oklahoma
100 N. Univ. Dr.
Edmond, Oklahoma 73034
USA
405-974-5473, 405-974-3812, elemley@uco.edu

Willy L. Duffle
Department of Engineering and Physics
University of Central Oklahoma
100 N. Univ. Dr.
Edmond, Oklahoma 73034
USA
405-974-5473, 405-974-3812, wduffle@uco.edu

Jesse K. Haubrich
Department of Engineering and Physics
University of Central Oklahoma
100 N. Univ. Dr.
Edmond, Oklahoma 73034
USA
405-974-5473, 405-974-3812, jhaubrich@uco.edu

Andrew W. Henderson
Department of Engineering and Physics
University of Central Oklahoma
100 N. Univ. Dr.
Edmond, Oklahoma 73034
USA
405-974-5473, 405-974-3812, ahenderson15@uco.edu

ABSTRACT

Laminar flow is increasingly important area of study as it dominates microscale and milliscale applications in devices such as microvalves, pumps, and turbines and in biomedical applications such as stents and biological flows. Studies of pressure losses in junctions have mostly been focused on turbulent flow conditions that exist in larger scale piping systems. There is a need for laminar flow studies of energy losses in junctions so that engineers can better predict, design, and analyze flow in microscale and other small scale systems. Unlike in the turbulent regime, Reynolds number plays a dominant role in energy losses for laminar flow, so new studies should document the effects of Reynolds number.

This paper documents laminar flow experiments in a milliscale junction. This work builds on previous experience of the authors in computational fluids dynamics simulations of junctions. The planar junction under study consists of a circular tubes with two outlets and one inlet. A general technique has been developed to produce computer and physical models of junctions in which the inlet tube size is set, but the outlets are allowed to vary in size and angle relative to the inlet tube. A generalized algorithm has been implemented to create three-dimensional models of the junctions for both computational and experimental studies. The junction test sections for experiments are milled from cast acrylic in two pieces to match three-dimensional computer models. The test sections are placed in a system that provides steady-state flow of water to test sections and has been designed to measure pressure losses and flow rates through the test section.

INTRODUCTION

Microfluidic flow networks and flow in porous networks are of interest in many engineering applications. These networks consist of interconnected tubes and channels and have numerous applications in pore networks [1-7] as well as in micro-power generation, biomedical use, computer chips, chemical separation processes, micro-valves, micro-pumps, and micro-flow sensors [8-10]. Many of these manufactured micro-channels are planar in nature, such as the micro-channel pressure sensor described by Lee et al [8]. Due to the size of these ducts and fluid properties, flow is usually laminar or transitional [9].

Systematic studies to address the issue of pressure losses in arbitrary bifurcations, such as that shown in Fig. 1, have not been published, although these type of splits are common in applications [1-10]. Published research about bifurcations (dividing flow) has focused on turbulent flow in either "t" geometries [11-15] or on standard "y" geometries [16]. Laminar dividing flow has received very little attention, since flow in large scale systems is often turbulent. Laminar loss coefficients in elbows, expansions, and reductions have been found by Edwards et al. [17] to be significantly larger than turbulent values, and highly dependent on Reynolds number.

The results are intended to allow analysis and design where laminar dividing flow exists. Examples of the use of such data are the design or analysis of microfluidic devices, the analysis of planar artificial flow networks (as described above), and the analysis and simulation of porous media using pore network models [1]. The loss coefficients for these bifurcations should allow one to analyze any type of flow condition including cases of different mass flow ratios, for example if one outlet is blocked or partially blocked to flow. Blockage may be accommodated by accounting for the loss coefficient's dependence on the fraction of total mass flow, f_i, that goes to each outlet duct.

NOMENCLATURE

d_1, d_2, d_3	=	duct diameters, as seen on Fig. 1 (m)
f_i	=	mass flow of duct i divided by inlet duct mass flow (-)
K_i	=	stagnation loss coefficient in outlet duct i (-)
L_i	=	distance from pressure sensor to test section inlet or exit
L_e	=	entrance length (m)
p_i	=	pressure at location i (Pa)
$\Re_d$	=	Reynolds number based on diameter and mean velocity (-)
u_i	=	velocity in duct i (m/s)
U	=	mean velocity in duct (m/s)
x, y	=	spatial coordinates

Greek characters

θ_i	=	angle between the inlet duct axis and the axis of the outlet duct i, as seen in Fig 1 (°)
μ	=	viscosity [kg/(m*s)]
ρ	=	density (kg/m^3)

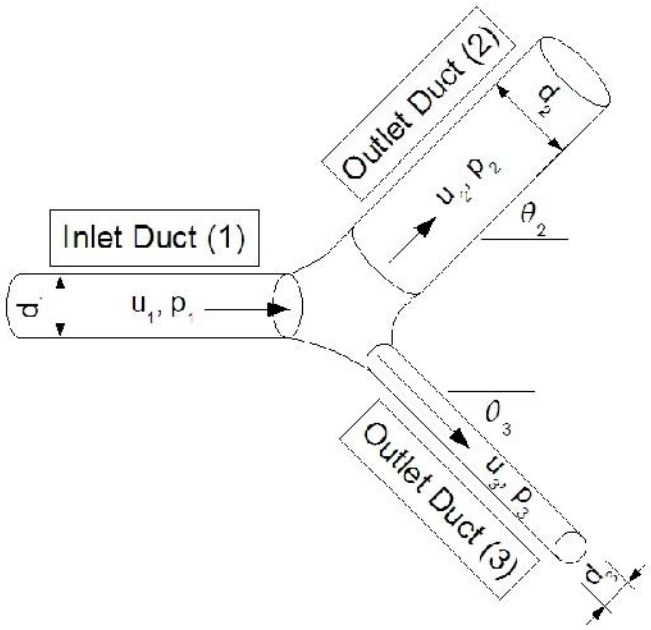

FIGURE 1. The general arrangement for the dividing flow simulations is shown with important geometric parameters.

PROBLEM DESCRIPTION

The problem addressed herein is depicted in Fig. 1 and involves finding the stagnation pressure loss coefficient for a particular planar geometry specified by the inlet and outlet duct diameters (d_1, d_2, and d_3) and the exit duct angles relative to the inlet duct direction: θ_2 and θ_3. The stagnation pressure loss coefficient in the i^{th} branch in Fig. 1 is defined as

$$K_i = \frac{\left(\frac{p_1}{\rho} + \frac{u_1^2}{2}\right) - \left(\frac{p_i}{\rho} + \frac{u_i^2}{2}\right)}{\frac{u_1^2}{2}} \quad (1)$$

The following flow conditions are parameters: inlet duct velocity (u_1) and inlet pressure (p_1) and the fraction of flow going to each exit duct (f_2 *and* f_3).

The work described here is an initial attempt to experimentally verify Computational Fluid Dynamics (CFD) results of flow in junctions. These previous CFD results are documented in Lemley et al. [18].

SOLUTION METHODOLOGY

Experimental System

A diagram of the experimental system used is shown in Fig. 2 and an image of the system is shown in Fig. 3 . The flow to a test section is provided by means of a constant head tank and a long entry tube containing a flow straightener. The

constant head tank is fed from an upper reservoir through a control valve to allow for various tank heights. The upper reservoir is fed through a small centrifugal pump from a sump tank. The flow leaving the test section is routed through two valves to control the flow fraction and Reynolds number of the flow in the entry tube.

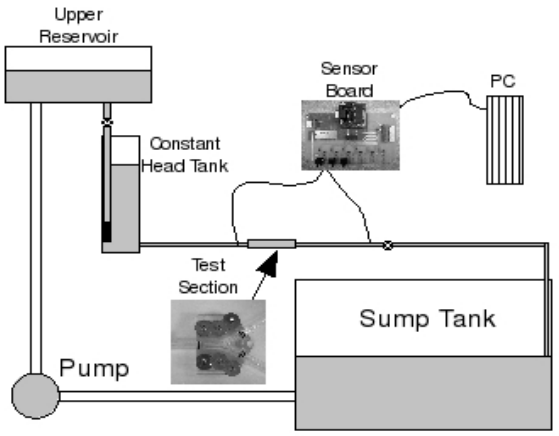

FIGURE 2. The overall experimental flow system.

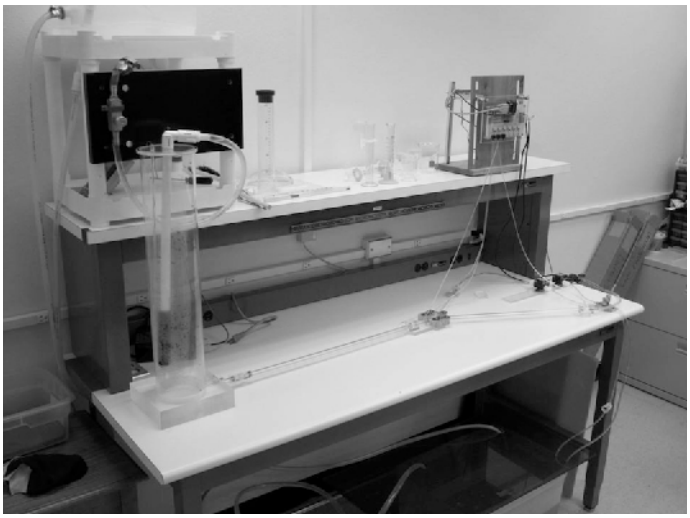

FIGURE 3. Image of the experimental flow system.

Pressure taps are located in-line upstream and downstream of the test section. Flexible tubing is routed from the taps to the flow sensors mounted on a printed circuit board.

Static pressure measurements are accomplished by means of differential pressure transducers (freescale™ MPVZ5004G) mounted to a custom made printed circuit board. These piezoresistive sensors have a range up to 3.92 kPa (differential). The sensors are driven to acquire data by a Parallax™ Basic Stamp 2 microprocessor through a Texas Instruments 12-bit Analog to Digital Converter (TLC2543). The Basic Stamp 2 is connected by serial cable to a personal computer, which runs custom Ruby software, named *fluidterm*, that controls data acquisition from the sensors through the Basic Stamp 2. The sensor output is filtered through a low pass filter so that sensor output is ± 1 mV for a constant pressure input. This allows pressure measurement with a resolution of ± 3 Pa.

The pressure sensor voltage output is linear within the stated range and allow for calibration slopes and intercepts to be determined using a water column of known height. These calibration results are used in fluidterm data acquisition code to calculate pressures from sensor voltage output.

The pressures are not measured at the inlet and exits of the test section so the measured differential pressure is corrected for frictional losses prior to and after a test section. The tube diameter entering or leaving a test section is the same diameter as the test section channels. The frictional losses are laminar and are corrected by

$$\Delta p_{friction} = \frac{64}{\Re} \frac{L_i}{d_i} \frac{\rho u_i^2}{2} \tag{2}$$

where

$$\Re = \frac{\rho u_i d_i}{\mu} \tag{3}$$

The distance from the tank exit to the upstream pressure tap is much longer than the laminar entrance length [19] as specified by

$$L_e = 0.06 \Re d_1$$

The distance from the head tank to the upstream pressure tap is over 150 diameters. From previous CFD simulations of flow in junctions [18], it is known that the flow leaving the test section is not fully developed, but that the distances to pressure taps in the exit ducts are 82 and 91 diameters respectively. These distances are long enough to assure the flow is fully developed at each downstream pressure tap.

In making measurement corrections in the way described above the resulting loss coefficients are *system* loss coefficients that reflect the presence of a junction on the pressure in terms of how it affects the system pressure.

Test Section Production

A robust process to create test sections has been developed that makes use of custom and commercial software to allow creation of junction test sections where geometry parameters (θ_i and d_i/d_1) can be varied considerably. The process begins by generating a computational model of a junction where θ_i can be varied from 5° to 90° and diameter ratios d_i/d_1 as small as 0.25 and as large as 5.0 can be chosen. This range of flexibility allows for a number of junctions to be created. Fig. 4 shows a sample junction.

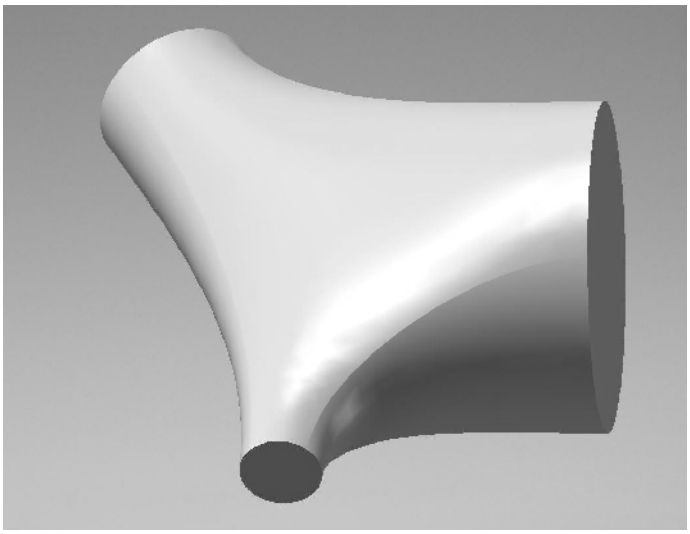

FIGURE 4. Sample junction used for simulations and test section production.

The computational junction model creation is completely automated for any number of junctions and allows batch processing of any number of junction models. The automation is achieved by custom software written in C++ dubbed *junction_code*. Code *junction_code* initially creates the junction in CAD software SolidWorks™, by modifying a code segment written in Microsoft Visual Basic for Applications (MS-VBA) that creates an initial computational model. This computational model is imported into CFD meshing software GAMBIT and *junction_code* (through a GAMBIT programming interface) adds inlet and exit tubes to the solitary junction model and names inlet, exits, and other features for CFD post-processing. At this point the junction model can be either readied for CFD runs in FLUENT or prepared for construction of a physical test section. A junction that is intended for CFD simulations is meshed and brought into FLUENT for runs as well as other post-processing.

A junction that is intended for a test section is manually imported into SolidWorks™ so additional features can be added. As a result of the process the junction, despite its geometric complexity, will be identical whether for simulations or experiments. The process to create a test section depends on what method of manufacturing will be used. The most common is to use a computer controlled mill (Roland® MDX 650A) to mill two pieces of acrylic that sandwich together to form a seamless test section. Figure 5 shows a junction that was manufactured in this way. Note there are channels that parallel the junction to allow manufacturing of a silicone gasket to make the test section leak free.

A tee geometry has been produced from milled acrylic as well. Attempts have been made to produce one piece junctions with other techniques. Junctions identical to that shown in Fig. 5 have been produced using a 3D printer and stereo lithography (SL). The SL junctions shown in Figs. 6-7 are microjunctions with inlets and exits all less or equal to 1 mm.

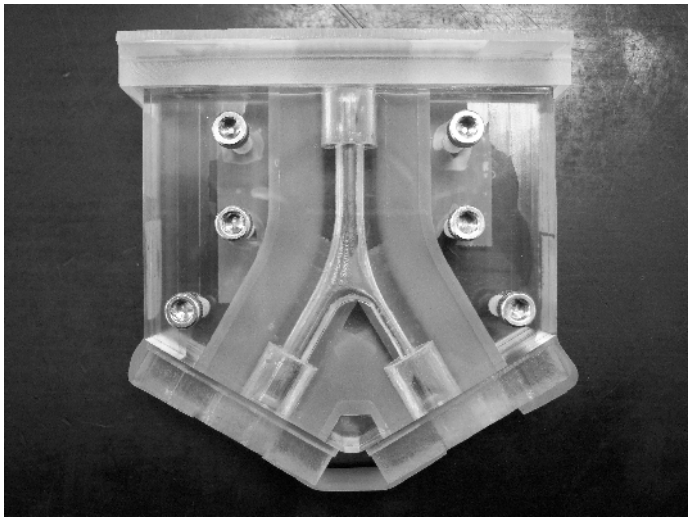

FIGURE 5. Milled acrylic test section.

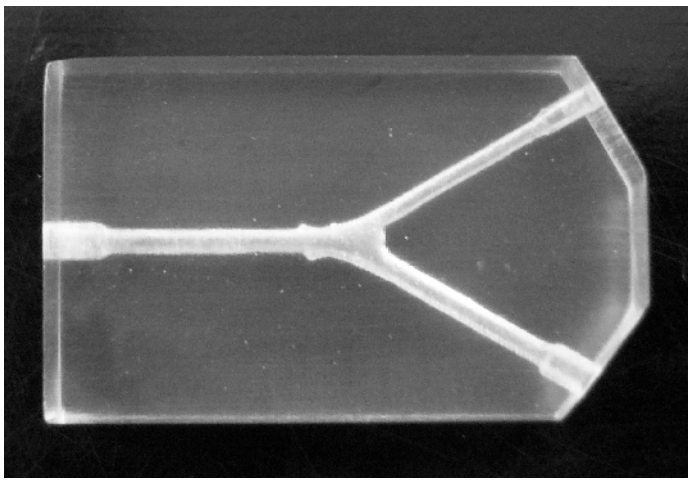

FIGURE 6. Scaled-down version of the junction shown in Fig. 4 produced by stereolithography. The inlet and exit tube on the bottom are 1 mm in diameter and the exit tube on top is 0.75 mm.

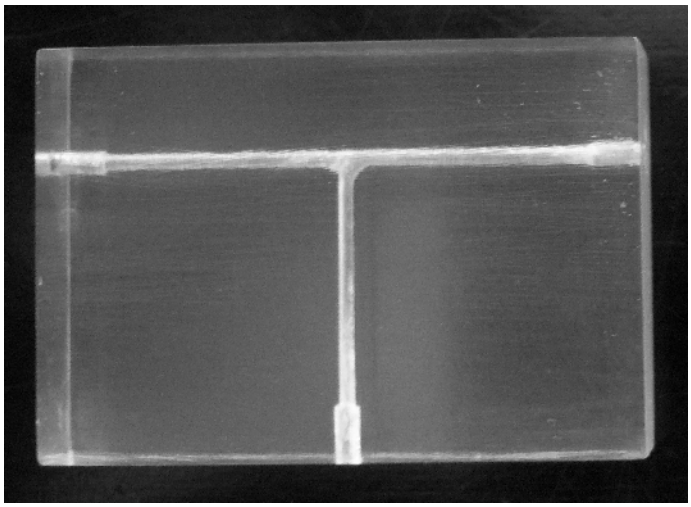

FIGURE 7. Scaled-down version of a tee junction produced by stereolithography. The inlet and exit tubes are all 0.75 mm.

Data Collection

In the experiments presented here deionized water 20-22°C has been used. The density was measured by collecting volumes of the water in a graduated cylinder using very small pipettes to ensure the volume was known to high precision. The masses of each collected volume was obtained using a digital balance to within 0.1 g. The resulting density was 980 ± 3 kg/m^3. The viscosity was measured using a Cannon™-Fenske Routine Viscometer and was found to be (9.40±0.04)x10^{-4} kg/m/s.

To date one junction has been used in experiments. This junction has $\theta_2 = 30^\circ$, $\theta_3 = 30^\circ$, $d_2/d_1 = 0.5$, and $d_3/d_1 = 1.0$. The inlet diameter $d_1 = 6.35\text{x}10^{-3}$ m. The constant head tank was kept at near 41 cm of water while the needle valves on the two junction exits were opened and closed to create a variation in Reynolds number and flow fractions. The system was steadied for a given flow condition by adjusting the needle valve on the inlet to the head tank.

Pressure measurements were made over a several minute period and controlled by the *fluidterm* program. Measurements were made at steady-state and after pressure sensors were zeroed for static conditions in the system. The average and standard deviation of the pressure were calculated for each sensor over the run time period. Flow rates are made during each run by measuring the mass of a collected volume of water for each exit branch and measuring the collection time. The measured water density is then used to calculate the collected volume, and the collection time is used to obtain volume flow rate for each branch.

The pressures, flow rates, and associated uncertainties are entered into a spreadsheet where a number of calculations are carried out resulting in a value for the stagnation loss coefficient, K_i, for each branch. Uncertainties are propagated through the calculations to yield the total experimental uncertainty in K_i.

RESULTS

Figures 8 and 9 show the measured stagnation loss coefficients for both sides of the junction. The loss coefficients in Figure 8 are for the case where the outlet duct is the same size as in the inlet duct. The range of Reynolds number on this plot is from 90 to 2100. Over that range there appears to be a significant drop in K_i from about 10 to 1.2. This is consistent with laminar loss coefficients for elbows and reductions as in Edwards et al. [17]. In Figure 9 the Reynolds number varies from 1000 to 2100 for the case where the exit duct is 50% of the inlet diameter. Over this range there is only a small change loss coefficient from 1.8 to about 5. A preliminary CFD result at the higher Reynolds numbers confirms a stagnation loss coefficient of about 5 at Reynolds of 2000. It is anticipated when smaller Reynolds numbers are run for this case that a similar result as in Fig. 8 will result.

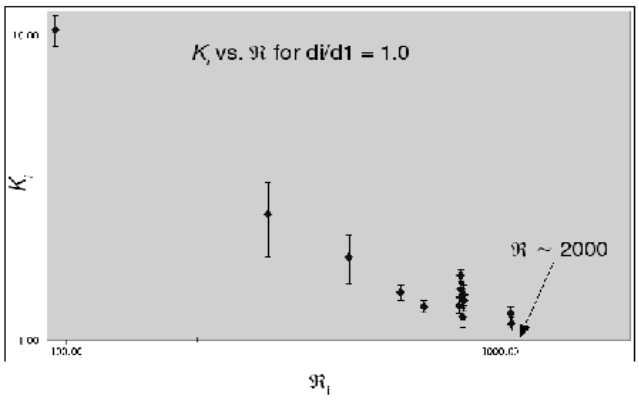

FIGURE 8. Results for stagnation loss coefficient versus Reynolds number for case of d_i/d_1 of 1.0. The error bars indicate the overall experimental uncertainty.

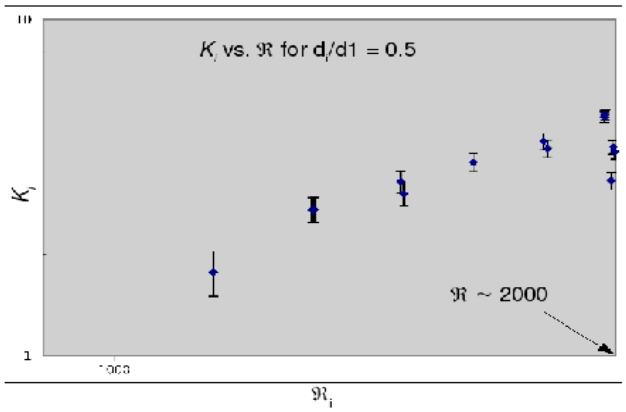

FIGURE 9. Results for stagnation loss coefficient versus Reynolds number for case of d_i/d_1 of 0.5. The error bars indicate the overall experimental uncertainty.

CONCLUSIONS

A system capable of measuring very small pressure differences in milliscale junction test sections as shown in Fig. 1 has been constructed and tested. A method to create arbitrary three-dimensional models of these junctions has been developed as well as techniques for creating micro-scale versions of these junctions. Initial experiments have been conducted to find the stagnation loss coefficient as a function of Reynolds number for a junction using the experimental system. The measured loss coefficients have expected behavior (based on other published laminar loss coefficients such as Edwards et al. [17]) for Reynolds number between 100 and 2000 as they decrease considerably from 100 to around 1000, then appear to flatten out to a constant value. Additional experiments with the system described are ongoing as well as CFD simulations of the Reynolds number dependence of loss coefficients in arbitrary junctions. The experimental results are intended to provide verification of full parameter variation CFD results.

ACKNOWLEDGMENTS

The Office of Research and Grants at the University of Central Oklahoma is acknowledged for support of this research. The Donors of The Petroleum Research Fund, administered by the American Chemical Society, are also be acknowledged for support of this research through grant PRF# 47193-B9. The National Science Foundation EPSCoR Research Opportunity Award Program is acknowledged in partial support of this research.

REFERENCES

1. Lao, H-W, Neeman, H.J., and Papavassiliou, D.V., 2004, "A Pore Network Model for the Calculation of Non-Darcy Flow Coefficients in Fluid Flow through Porous Media," Chem. Eng. Com., **191**(10), pp. 1285-1322.
2. Lin C.-Y. and J.C. Slattery, 1982, "Three-Dimensional, Randomized, Network Model for Two-Phase Flow Through Porous Media," AIChE J., **28**(2), pp. 311-324.
3. Dias, M.M. and Payatakes, A.C., 1986, "Network Models for Two-Phase Flow in Porous Media. Part 1. Immiscible Microdisplacement of Non-Wetting Fluids," J. Fluid Mech., **164**, pp. 305-336.
4. Rajaram, H., Ferrand, L.A., and M.A. Celia, 1997, "Prediction of Relative Permeabilities for Unconsolidated Soils using Pore-scale Network," Water Resources Research, **3**(1), pp. 43-52.
5. Dahle, H.K., and M.A. Celia, 1999, "A Dynamic Network Model for Two-Phase Immiscible Flow," Computational Geosciences, **3**, pp. 1-22.
6. Thauvin, F., and K.K. Mohanty, 1998, "Network Modeling of Non-Darcy Flow Through Porous Media," Transport in Porous Media, **31**, pp. 19-37.
7. Lemley, E.C., Papavassiliou, D.V., and H.J. Neeman, 2007, "Non-Darcy Flow Pore Network Simulation: Development and Validation of a 3D Model," *Proceedings of FEDSM2007,* 5th Joint ASME/JSME Fluids Engineering Conference, paper FEDSM2007-37278.
8. Lee, W.Y., Wong, M., and Zohar, Y., 2002, "Microchannels in Series Connected Via a Contraction/expansion Section", J. Fluid Mech., **459**, pp.187-206.
9. Graveson, P., Branebjerg, J., and Jensen, O.S., 1993, "Microfluidics a Review," J. Micromech. Microeng., **3**, pp.168-182.
10. Judy, J., Maynes, D., and Webb, B.W., 2002, "Characterization of Frictional Pressure Drop for Liquid Flows Through Microchannels," Intl. J. Heat Mass Trans., **45**, pp.3477-3489.
11. Basset, M.D., Winterbone, D.E., and Pearson, R.J., 2001, "Calculation of Steady Flow Pressure Loss Coefficients for Pipe Junctions," Proc. Instn. Mech. Engrs., Part C, Journal of Mechanical Engineering Science, **215** (8), pp. 861-881.
12. W.H. Hager, 1984, "An Approximate Treatment of Flow in Branches and Bends," Proc. Instn. Mech. Engrs., Part C, Journal of Mechanical Engineering Science, **198**(4) pp. 63-9.
13. Blaisdell, F.W., and Manson, P.W., 1967, "Energy loss at pipe junctions," J. Irrig. and Drainage Div., ASCE, **93**(IR3), pp. 59-78.
14. Schohl, G.A., 2003, "Modeling of Tees and Manifolds in Networks," *Proceedings of the 4th ASME/JSME Joint Fluids Engineering Conference*, **2**, Part D, pp. 2779-2786.
15. Bassett, M.D., Pearson, R.J., and Winterbone, D.E., 1998, "Estimation of Steady Flow Loss Cofficients for Pulse Converter Junctions in Exhaust Manifolds," *IMechE Sixth International Conference on Turbocharging and Air Management Systems*, IMechE HQ, London, UK, **C554/002**, pp.209-218.
16. Ruus, E., 1970, "Head Losses in Wyes and Manifolds," J. Hyd. Div., ASCE, **96**(HY3), 593-608.
17. Edwards, M.F., Jadallah, M.S.M., and Smith, R., 1985, "Head Losses in Pipe Fittings at Low Reynolds Numbers," Chem. Engr. Res. Des., **63**(1), pp. 43-50.
18. Lemley, E.C., Papavassiliou, D.V., and H.J. Neeman, 2007, "Simulations To Determine Laminar Loss Coefficients In Arbitrary Planar Dividing Flow Geometries," *Proceedings of FEDSM2007,* 5th Joint ASME/JSME Fluids Engineering Conference, paper FEDSM2007-37268.
19. White, F., 2003, *Fluid Mechanics*, 5th Ed., McGraw-Hill, New York, pp. 277-322, Chap. 6.